

AD 632440

TECHNICAL REPORT NO. 577

INVISCID FLOW FIELD PAST A POINTED

CONE AT AN ANGLE OF ATTACK

PART I - ANALYSIS

By G. Moretti

CLEARINGHOUSE
FOR FEDERAL SCIENTIFIC AND
TECHNICAL INFORMATION

Hardcopy

Microfiche

\$ 2.00

\$ 0.50 / 5 pp

ARCHIVE COPY

Co-cc 1

December 15, 1965

RESEARCH
ENGINEERING
PRODUCTION

Project 8030/0650

Total No. of Pages - iv and 40

Copy (12) of 125

TECHNICAL REPORT NO. 577

INVISCID FLOW FIELD PAST A POINTED

CONE AT AN ANGLE OF ATTACK*

PART I - ANALYSIS

By G. Moretti

Prepared for

Advanced Research Projects Agency
Washington, D. C.

Under Contract SD-149, Supplement No. 6
ARPA Order No. 396
Project Code 3790

"Ballistic Reentry Studies"

Project Engineer - Dr. H. Lien
Code 516 - 333-6960

Prepared by
General Applied Science Laboratories, Inc.
Merrick and Stewart Avenues
Westbury, L. I., New York

December 15, 1965

Approved by:


Robert W. Byrne
Vice President

*This research is sponsored by the
Advanced Research Projects Agency.

SUMMARY

The conical inviscid flow field past a circular cone at an angle of attack is obtained as the asymptotic stage of a three-dimensional flow. The latter is computed in a spherical frame by means of finite difference techniques associated with a method of characteristics on the shock and body. A brief critical discussion of previous papers on the subject and an analysis of the numerical results are given. Comparison with experiments shows that the applicability of the theory is severely limited by boundary layer effects.

TABLE OF CONTENTS

<u>SECTION</u>	<u>TITLE</u>	<u>PAGE</u>
I	INTRODUCTION	1
II	THE CENTRAL IDEA FOR A NEW TECHNIQUE	4
III	DETAILS OF THE ANALYSIS	7
IV	THE COMPUTATION OF THE THREE- DIMENSIONAL FLOW FIELD, INNER POINTS	15
V	COMPUTATION OF THE SHOCK WAVE	18
VI	COMPUTATION OF POINTS ON THE BODY	20
VII	RESULTS AND DISCUSSION	22
VIII	LIMITATIONS OF THE INVISCID MODEL	26
	References	27
	Table I	29
	Figures	30

LIST OF FIGURES

<u>Figure No.</u>	<u>Title</u>	<u>Page</u>
1	Schematic of Cone and Assumed Shock Geometry	30
2	Schematic of Mesh	31
3	Range of $\Delta\theta/\Delta r$ as a Function of Radius	32
4	Mass Flow as a Function of Radius	33
5	Velocity Distribution in Symmetry Plane Determined from Computed Values of W_{ϕ}	34
6	Assumed and Computed Entropy Distribution	35
7	Entropy Distribution on Body at Various Values of r/r_0	36
8	Pressure Distribution Case 1	37
9	Pressure on Body, $M_{\infty} = 8$, $\epsilon = 20^\circ$, $\alpha = 5^\circ$	38
10a	Computed Shock Shapes for Cases 1, 2	39
10b	Computed Shock Shapes for Cases 3,4	40

TECHNICAL REPORT NO. 577

INVISCID FLOW FIELD PAST A POINTED

CONE AT AN ANGLE OF ATTACK

PART I - ANALYSIS

By G. Moretti

I. INTRODUCTION

The State of the Art

The steady supersonic flow past a pointed cone of revolution at zero angle of attack was first studied by Busemann in 1929, and by other authors in the thirties (Ref. 1). The definition of a conical flow was given as that of a flow whose parameters do not depend on r in a spherical frame of reference, (r, θ, φ) . As a matter of fact, the flow past a pointed cone of revolution at zero angle of attack is also axisymmetric, that is, its parameters do not depend on φ either. The latter problem is reduced to solving two ordinary differential equations, with θ as the only independent variable:

$$\begin{cases} du/d\theta = v \\ dv/d\theta = -u + (u + v \cot \theta)/(v^2/a^2 - 1) \end{cases} \quad (1)$$

(the three velocity components in the spherical frame being u , v , and w , respectively, and a being the speed of sound). In 1947, such equations were coded for an electronic computer by Kopal and his staff (Ref. 2), and the results tabulated. Today, Kopal's tables are obsolete, since a program of not more than 20 FORTRAN statements may provide a direct evaluation of the flow, once the free-stream Mach number, the semi-angle of the cone, ϵ , and the ratio of specific heats, γ , are given.

In the late forties, the problem of a pointed cone at an angle of attack, α , was considered, with some optimism, to be a simple extension of the case above, at least for $\alpha \ll \epsilon$. It is easy to prove that a steady conical flow may exist, whose parameters depend on θ and ϕ . Five differential equations are needed now (since, in addition to u and v , the third velocity component, w , the pressure, p , and either the density, ρ , or the entropy, S , must be determined), but the independent variables number only two. In fifteen years, several attempts have been made to solve the problem so formulated, and the number of papers is so large that an exhaustive list cannot be given here.

The problem proved to be a very tough one, since the system of equations which describes it is elliptic, if α is small and $v^2 + w^2 < a^2$, and becomes of the mixed type for larger values of α , if there are regions of the (θ, φ) -sphere in which $v^2 + w^2 > a^2$. In such a sphere, the shape of the cone is given, but the shock wave is unknown. In this respect, the problem of a cone at an angle of attack is similar to the blunt body problem, and similar techniques have been used in both problems, such as inverse methods with step-on integration from the shock to the body (Ref. 3), methods of integral relations (the "strip-method" of Belotserkovsky) (Ref. 4), and methods of series expansions (Ref. 8). In the latter case, some papers try to improve the original linearized formulation of Stone (Refs. 5,6) and Ferri (Ref. 7), others (Refs. 9,10) are related to Chernyi's expansion in powers of $(\gamma-1)/(\gamma+1)$, etc.

II. THE CENTRAL IDEA FOR A NEW TECHNIQUE

Critical objections, similar to the ones discussed in some detail for the blunt body problem (Ref. 11), may be raised here. Briefly, since a numerical procedure is used to solve the problem, a system of elliptic equations is ill-suited for the job. In the blunt body problem, a powerful and accurate technique may be set up if the system is made hyperbolic by considering the steady state as the asymptote of an unsteady one. In the present problem, the equations of a steady flow in the three coordinates, r , θ , and φ , form a hyperbolic system. Consequently, the problem is easier to handle if the motion is not conical. Let us consider, then, the conical motion as the asymptote (with respect to r) of a non-conical one. To this effect, assume an arbitrary set of initial conditions on a sphere, $r = r_0$, say, and compute the flow from there on as dependent on θ , φ , and r , until an asymptotic state, independent of r , develops. The physical argument for the existence of a conical flow as an asymptotic one is that the flow in the shock layer is forced by the outer flow, which is uniform (and therefore conical) and the geometry of the body (which is a cone).

In the present approach an initial value of r is defined, and we suppose that the asymptotic values are reached at another value of r , $r = r_1$, say. The difference, $r_1 - r_0$, represents the actual length which the flow should travel in order to overcome the initial state (a perturbed, non-conical one) with a continuous build-up of conical effects. Such a length will obviously be the longer, the farther the initial conditions are from a conical flow. But the length itself is immaterial, since no length is involved in a conical flow. One can think in terms of the perturbation being confined to such a small region in the vicinity of the apex that the distance $r_1 - r_0$ itself is as small as we please. (After all, what is a pointed cone from a physical point of view, if not a blunted cone whose blunt, irregular, discontinuous nose is detectable only with a microscope?)

As a matter of fact, the building up of a conical flow around a blunted cone, such a flow being similar to what should be expected in a pointed cone, has been investigated experimentally (Ref. 12) and numerically (Ref. 13). The conclusion was that after about ten nose radii from the tip of the cone a conical flow is well established. However, the high entropy

layer consequent to the central portion of the bow shock fills a significant portion of the shock layer. The entropy pattern, then, is not what is expected from a theoretical analysis of a pointed cone, and an independent numerical analysis is still considered necessary.

III. DETAILS OF THE ANALYSIS

The Initial Conditions

The present analysis differs from the one mentioned in the previous section (Ref. 13) in the choice of the initial conditions and in the technique used to solve the three-dimensional equations of a steady flow.

As said before, it is convenient to choose the initial conditions as close as possible to the solution for the conical flow, since the computational time will be reduced to a minimum. Moreover, we do not want to start with a set of values consistent with a blunt body calculation, since we want to avoid the after effects of a high entropy layer. The initial values are guessed as follows:

It is assumed that the trace of the shock on a plane, normal to the axis of the cone, is an ellipse if the angle of attack $\alpha \neq 0$. We consider such a plane as tangent to the unit sphere, whose center is the apex of the cone, and also assume that, within the shock layer, $r \cong \tan \theta$. Therefore in Fig. 1, where the plane is represented, the spherical θ -coordinate of any point is equal to the distance between such a point and the origin, O . In this figure, O is the

trace of the axis of the cone ($\theta = 0$), V is the trace of the vector, parallel to V_∞ , through the apex of the cone, E is the center of the shock ellipse, δ_1 and δ_2 are the angles between shock and body in the leeward and windward side respectively, A and B are the semi-axes of the ellipse, ϵ is the angle between shock and body on the x-axis, and b is the semi-angle of the cone. Note that

$$\epsilon = A \sqrt{1 - C^2/B^2} - b \quad (2)$$

First, the conical flow consistent with the assigned cone at no incidence is computed, and a value, δ_0 , of the angle between shock and body in the plane of Fig. 1 is obtained. It is then postulated that

$$(\epsilon + \delta_2)/2 = \delta_0 \quad (3)$$

independent of the Mach number and the angle of attack (such an assumption is well justified by experimental results).

From (2) and (3) A may be expressed as a function of B and C ,

$$A = \frac{C - B + 2b \pm 2\delta_0}{\sqrt{1 - C^2/B^2}} \quad (4)$$

Consequently, only two parameters, B and C, are left to define the ellipse. They are related to δ_1 and δ_2 through the equations,

$$\begin{aligned} B &= b + (\delta_1 + \delta_2)/2 \\ C &= (\delta_1 - \delta_2)/2 \end{aligned} \tag{5}$$

On the plane of symmetry, $w = 0$ and the derivatives of u , v , and p with respect to φ also vanish. If a conical motion is assumed, the equations of motion in such a plane reduce to the simple form,

$$\begin{aligned} u_\theta &= v \\ v_\theta &= -u + (u + v \cot \theta + w_\varphi / \sin \theta) / (v^2/a^2 - 1) \end{aligned} \tag{6}$$

where a subindex means differentiation with respect to that variable.

Note that the only difference between (1) and (6) is the presence of the term $w_\varphi / \sin \theta$ in the latter. Therefore, the same technique used to determine the conical flow at no incidence could be applied to solve (6), if $w_\varphi / \sin \theta$ were known as a function of θ . Since we do not know it, we assume

that w_φ is constant between M and N and between P and Q.

Let s be the value of θ at the shock. From the equation of the ellipse, and letting $\theta = \tan \theta$, $r_0 = 1$, it follows that

$$s = \frac{C \cos \varphi + B \sqrt{(B^2 - C^2)/A^2 \sin^2 \varphi + \cos^2 \varphi}}{(B/A)^2 \sin^2 \varphi + \cos^2 \varphi}$$

and

$$s_{\varphi\varphi} = -BC (C \pm 2B)/A^2 \quad (8)$$

at the symmetry plane, where the upper sign holds between M and N and the lower one between P and Q. From the Rankine-Hugoniot equations,

$$w_\varphi = Us_{\varphi\varphi} / \sin s - V_\varphi \quad (9)$$

where U is the component of the velocity behind the shock along the normal to the shock wave, pointing inwards, and V_φ is the derivative with respect to φ of the component of the velocity along the tangent to the shock wave in the plane of Fig. 1. The component of the velocity in front of the shock along the normal is

$$V_\infty \sin (s \mp \alpha) \quad (10)$$

where V_∞ is the velocity at infinity and with the upper sign for point N and the lower one for point Q. From (10), U is obtained through the Rankine-Hugoniot equations. From the same equations,

$$V_\varphi = V_\infty [s_{\varphi\varphi} \cos \alpha \pm (1 - s_{\varphi\varphi} \cot s)] \quad (11)$$

We have now the equations which are necessary and sufficient to determine B and C. From a computational point of view, an iteration procedure is convenient and is used. Two values of B and C are guessed, the corresponding values of w_φ on the leeward and windward sides are evaluated, then the system of Eqs. (6) is integrated between N and M and between Q and P. Two new values of δ_1 and δ_2 result, from which two new values of B and C are obtained, and the procedure is repeated until (after three or four iterations) the solution is obtained.

At this stage, a number of equally spaced meridional planes ($\varphi = \text{constant}$) is considered and, along the intersection of each plane with the unit sphere, a number of equally spaced points is taken between the cone and the shock, (left-hand side of Fig. 2).

The auxiliary variable ζ is introduced, defined by

$$\zeta = \frac{\theta - b}{\delta} \quad (12)$$

where

$$\delta = s - b \quad (13)$$

The shock layer is thus mapped onto a rectangle in a (Y, ζ) -plane, where $Y = \varphi$. (right-hand side of Fig. 2). The initial values of u , v , w_φ , p , and ρ are known at the points on the lines $Y = 0$ and $Y = \pi$, from the computation outlined above. The shock shape, $s = s(\varphi)$ is known as an ellipse and, since we assumed that $s_r = 0$ (conical flow), its geometry in space is completely defined. The Rankine-Hugoniot equations can be applied at any point on the shock ($\zeta = 1$), to determine the physical properties behind it, that is, u , v , w , p , and ρ . On the body ($\zeta = 0$), $v = 0$,

$$2R = R(0,0) + R(\pi,0) + [R(0,0) - R(\pi,0)] \cos \varphi$$

$$2P = P(0,0) + P(\pi,0) + [P(0,0) - P(\pi,0)] \cos \varphi \quad (14)$$

$$2w = \{w_\varphi(0,0) - w_\varphi(\pi,0) + [w_\varphi(0,0) + w_\varphi(\pi,0)] \cos \varphi\} \sin \varphi$$

where

$$\begin{aligned} R(Y, \zeta) &= \ln(\rho/\rho_\infty) \\ P(Y, \zeta) &= \ln(p/p_\infty) \end{aligned} \quad (15)$$

and u is obtained from the definition of the total enthalpy.

Note that, since the entropy, S , is given by

$$S = P - \gamma R \quad (16)$$

(within a constant factor, c_v), it follows that the initial entropy on the body is distributed with a simple trigonometric law.

The values of v , w , P , and R at the interior points of the grid in the (Y, ζ) -plane are linearly interpolated between body and shock and, again, u is obtained from the definition of the total enthalpy.

At this stage, a slight correction on the values of ρ (and, consequently, of R) at the interior points is made, in order to match the total mass-flow between shock and body with the mass-flow of the uniform stream through the elliptic section of the unit sphere,

$$m_\infty = \rho_\infty V_\infty \int_0^\pi d\varphi \int_0^S (\cos \alpha \cos \theta + \sin \alpha \sin \theta \cos \varphi) \sin \theta d\theta \quad (17)$$

Let ρ_0 and u_0 be the values of ρ and u as computed above, and

$$\rho = \rho_0 + \eta \zeta(1 - \zeta) \quad (18)$$

where η is a constant, $\eta \ll 1$. Then the mass-flow between shock and body is

$$m = \int_0^\pi \delta(\varphi) d\varphi \int_0^1 [\rho_0 + \eta \zeta(1 - \zeta)] (u_0 + \eta u_1) \sin \theta d\theta \quad (19)$$

where u_1 is the first order correction to u as obtained from the expression of the total enthalpy,

$$u_1 = \frac{\gamma p \zeta(1 - \zeta)}{(\gamma - 1) \rho_0^2 u_0} \quad (20)$$

Consequently

$$\begin{aligned} m &= \int_0^\pi \delta(\varphi) d\varphi \int_0^1 \rho_0 u_0 \sin \theta d\theta \\ &+ \eta \int_0^\pi \delta(\varphi) d\varphi \int_0^1 \zeta(1 - \zeta) \left[u_0 + \frac{\gamma p}{(\gamma - 1) \rho_0 u_0} \right] \sin \theta d\theta \quad (21) \\ &= m_1 + \eta m_2 \end{aligned}$$

and, since $m = m_\infty$

$$\eta = \frac{m_\infty - m_1}{m_2} \quad (22)$$

IV. THE COMPUTATION OF THE THREE-DIMENSIONAL FLOW FIELD. INNER POINTS

The computation of the non-conical flow subsequent to the initial conditions is performed along the same general lines described for the blunt-body problem (Ref. 11). An auxiliary space (T, Y, ζ) is used, where Y and ζ have been defined above, and $T = r$. Referring to the right-hand side of Fig. 2, one can imagine a T -axis normal to the plane of the figure. The grid does not change with T .

Letting

$$\begin{aligned} q &= \ln(u/V_\infty) \\ \sigma &= v/u \\ \tau &= w/u \end{aligned} \quad (23)$$

the equations of motion in the new coordinates are

$$\begin{aligned} R_T + q_T &= - [AR_\zeta + BR_Y - \zeta s_r q_\zeta / \zeta + v_\zeta / ru\delta \\ &\quad + (w_Y - \zeta s_\phi w_\zeta / \delta) / ru \sin \theta + (2 + \sigma \cos \theta) / r] \\ (a^2/u^2)R_T + q_T &= - [Aq_\zeta + Bq_Y - a^2 \zeta s_r R_\zeta / u^2 \delta - (a^2/\gamma u^2) [(\sigma/r \\ &\quad - \zeta s_\phi B) S_\zeta / \delta + BS_Y] - (\sigma^2 + \tau^2) / 2] \end{aligned} \quad (24)$$

$$\begin{aligned}
 v_T &= - [Av_\zeta + Bv_Y + a^2 P_\zeta / \gamma r u \delta + (v - wT \cot \theta) / r] \\
 w_T &= - [Aw_\zeta + Bw_Y + (a^2 / \gamma r u \sin \theta) (P_Y - \zeta s_\phi P_\zeta / \delta) \\
 &\quad + (w + vT \cot \theta) / r] \\
 S_T &= - [AS_\zeta + BS_r]
 \end{aligned}
 \tag{24}$$

Cont'd

where

$$\begin{aligned}
 B &= \tau / r \sin \theta \\
 A &= (\sigma / r - \zeta s_r - \zeta s_\phi B) / \delta
 \end{aligned}
 \tag{25}$$

All points inside the grid (that is, neither at $\zeta = 0$ nor at $\zeta = 1$) are computed assuming that

$$g(T + \Delta T, Y, \zeta) = g(T, Y, \zeta) + g_T(T, Y, \zeta) \Delta T + g_{TT}(T, Y, \zeta) \Delta T^2 / 2
 \tag{26}$$

where g is any of the parameters g , v , w , R , and S . The system of Eqs. (24) provides the formal expressions for the first derivatives, g_T . The first derivatives with respect to Y and ζ , which appear in the right-hand sides, are evaluated by central differences. In addition, s_ϕ is obtained from the shape of the shock at T (how to obtain s_r is explained in the next section).

In order to obtain the second order derivatives, g_{TT} , each of Eqs. (24) is formally differentiated with respect to T . The

second order mixed derivatives, of the type $g_{T\zeta}$, g_{TY} which appear in the right-hand sides, are formally obtained again by differentiating the Eqs. (24) with respect to ζ and Y . In this way, the evaluation of the last term in (26) is reduced to computing 3-point centered second derivatives with respect to $\zeta\zeta$, ζY , and YY , and to some algebraic manipulations. Note that $\delta_T = s_r$.

The terms, s_{rT} , $s_{\phi T}$ are evaluated as

$$\frac{s_r(T + \Delta T, Y) - s_r(T, Y)}{\Delta T}, \quad \frac{s_\phi(T + \Delta T, Y) - s_\phi(T, Y)}{\Delta T}$$

Derivatives with respect to ζ and Y of complicated factors, such as A , $a^2/\gamma r u \sin \theta$, etc. are not formally evaluated, but computed by central differencing of the factors themselves.

The value of ΔT which can be used at each step is limited by a stability criterion. The well known Courant-Friedrichs-Lewy rule is applied, which forbids computing values at a point outside the domain of influence of the initial points (Ref. 16).

V. COMPUTATION OF THE SHOCK WAVE

The points on the shock wave are computed with an improved version of a technique successfully used in general three-dimensional flow field computations (Ref. 13).

The equations of motion in spherical coordinates are written moving all derivatives with respect to ϕ to their right-hand sides, and the third momentum equation is stricken out, so that the system looks as follows:

$$- S_r/\gamma - \sigma S_\theta/\gamma r + P_r/\gamma + \sigma P_\theta/\gamma r + q_r + v_\theta/ru = - [\tau R_\phi + w_\phi/u]/\sin \theta + 2 + \sigma \cot \theta]/r$$

$$(a^2/u^2) (-S_r/\gamma - \sigma S_\theta/\gamma r + P_r/\gamma) + q_r + \sigma q_\theta/r = [(a^2 S_\phi/\gamma u^2 - q_\phi) \tau/\sin \theta + \sigma^2 + \tau^2]/r$$

$$a^2 P_\theta/\gamma ru + v_r + \sigma v_\theta/r = [-v - \tau v_\phi/\sin \theta + w \tau \cos \theta]/r$$

$$S_r + \sigma S_\theta/r = - \tau S_\phi/r \sin \theta \quad (27)$$

In a (r, θ) -plane, this system has three characteristics, defined by

$$\lambda^I = r \frac{d\theta}{dr} = \frac{uv + a \sqrt{u^2 + v^2 - a^2}}{u^2 - a^2}$$

(28)

$$\lambda^{II} = r \frac{d\theta}{dr} = \frac{uv - a \sqrt{u^2 + v^2 - a^2}}{u^2 - a^2}, \quad r \frac{d\theta}{dr} = \sigma$$

The compatibility equation along the first characteristic reads

$$\begin{aligned}
 (a/\gamma u^2) \sqrt{u^2+v^2-a^2} \frac{dP}{dr} + \frac{d\sigma'}{dr} = & \left(\frac{\sigma}{r} - \lambda^I \right) (w_\phi/u \sin \theta + 2 \\
 & + \sigma \cot \theta) + \lambda^I (\tau q_\phi/\sin \theta - \sigma^2 - \tau^2) \\
 & - (\tau v_\phi/\sin \theta + v - wT \cos \theta)/ru \\
 & - \left(a\sigma + \sqrt{u^2+v^2-a^2} \right) P_\phi \tau a/\gamma r (u^2-a^2) \sin \theta
 \end{aligned}
 \tag{29}$$

By computing the coefficients and the right-hand side at a suitable initial point, the values of P and σ may match the values of P and σ computed from the Rankine-Hugoniot conditions, with a proper choice of s_r . By iteration, the matching values, including s_r , are easily computed.

VI. COMPUTATION OF POINTS ON THE BODY

A similar technique is used to compute points on the body.

The compatibility equation along the second characteristic,

$$\begin{aligned}
 (a/\gamma u^2) \sqrt{u^2+v^2-a^2} \frac{dP}{dr} - \frac{d\sigma}{dr} = & - \left(\frac{\sigma}{r} - \lambda^{II} \right) (w_\phi/u \sin \theta + 2 \\
 & + \sigma \cot \theta) - \lambda^{II} (\tau q_\phi/\sin \theta - \gamma^2 - \tau^2) \\
 & + (\tau v_\phi/\sin \theta + v - w\tau \cos \theta)/ru + \\
 & + \left(a\sigma \sqrt{u^2+v^2-a^2} \right) P_\phi \tau a/\gamma r (u^2-a^2) \sin \theta
 \end{aligned} \tag{30}$$

must be used. Again, the coefficients and the right-hand side are computed at a suitable initial point and the condition, $v = 0$ on the body, is used. Consequently, P is found at a body point. The fluid momentum equation then is used, in which $v = 0$:

$$\frac{1}{w} \frac{Dw}{Dt} = w_r + \frac{\tau}{r \sin \theta} w_\theta = - (w + a^2 P_\phi/\gamma u \sin \theta)/r \tag{31}$$

the last of Eqs. (27) reads now

$$\frac{1}{u} \frac{DS}{Dt} = S_r + \frac{\tau}{r \sin \theta} S_\phi = 0 \tag{32}$$

Both Lagrangian derivatives are taken along a streamline which wets the body. Thus, by finding the initial point on such a streamline and computing the pertinent values of w , S , and the

right-hand side of (31), the values of w and S at the point on the body may be evaluated. Finally, the value of u at the body point is obtained from the condition of constant total enthalpy.

At the body point in the leeward symmetry plane ($\varphi = 0$), however, the entropy is forced to be equal to the entropy of the neighboring point in the same plane. A similar policy is adopted for the body point in the windward symmetry plane ($\varphi = \pi$). The reason for it is that no streamline enters or leaves the symmetry planes. When the flow has settled down to a conical one, the entropy on each of these planes must be a constant. Our device allows the body points in the symmetry planes to adjust their entropies to the final entropies at the shock points, independent of the original guess.

VII. RESULTS AND DISCUSSION

The following sample problems have been run, in order to test the technique:

- (1) $M_\infty = 7.95, \epsilon = 10^\circ, \alpha = 8^\circ$
- (2) $M_\infty = 7.95, \epsilon = 10^\circ, \alpha = 4^\circ$
- (3) $M_\infty = 8, \epsilon = 20^\circ, \alpha = 5^\circ$
- (4) $M_\infty = 20, \epsilon = 30^\circ, \alpha = 10^\circ$

The first two cases were chosen to compare our results with Tracy's experiments (Ref. 14), the third one to conclude the discussion and to check with other experiments which were made in testing our three-dimensional flow field computations (Ref. 13), the fourth one to show the reversed situation (leeward side thinner than the windward side) which is to be found at high Mach numbers (Ref. 15). We will analyze the first case in detail.

It took four iterations to define the shape of the initial shock wave. Table I shows the values of B and C, their errors (that is, the differences between B and C at one step and B and C at the next step) and the corresponding values of w_ϕ in the leeward side (labeled 1) and the windward side (labeled 2). In the same table, values of u, v, ρ , p, M, and v/u are given as functions of θ in the symmetry plane (from the shock to the body). Note that all dimensional quantities are made nondimensional;

pressures and densities are divided by p_∞ and ρ_∞ respectively; velocity components are divided by $\sqrt{p_\infty/\rho_\infty}$. The subsequent computation was performed (in this as in the other cases) considering 11 meridional planes, spaced 18° apart, and 6 points in each plane (including the shock and body points).

As a result of the non-conical computation, the shock wave undergoes a deformation. The values of s_r , which are assumed as zero initially and should be identically zero in a conical flow, change with r and ϕ . If the flow sets down to a conical one, then s_r must vanish again identically. A first indication of the tendency of the flow toward a conical state may be found by plotting the range of values of s_r at each computed value of r . This is done in Fig. 3. Since s_r is of the order of .2, the shock shape may be considered as stabilized when s_r is of the order of 10^{-4} , and this situation occurs at step 200, $r \approx 13.6$, far before the end of the run, which was interrupted at step 540, $r = 1073$.

In Fig. 4 the internal mass-flow (across a spherical section of the shock layer at a given station) and the external mass-flow (across the whole shock wave from the apex to the same station) are plotted after having been divided by r^2 . It is clear again that a stable flow configuration is reached, after

about 400 steps (in a conical flow, m/r^2 is a constant). It is also interesting to note that the error (difference between internal and external mass flow) is of the order of $1/1000$ of the total mass flow).

There is a way of testing the soundness of the results. If the flow, as found by the present technique, is conical, then it is ruled by Eqs. (6) in the symmetry plane. Let us perform again the integration of such a system, starting from the shock as defined by the present technique and using what we assume are the correct values of $w_\varphi(\theta)$. The integration should give the correct value for the body angle and the distributions of u and v between shock and body should match the ones obtained with the present technique. This actually happens within three significant figures. The body angle, in radians, is .17453. The body angles computed from (6) with the values of w interpolated from the last step in our sample run are .17410 in the leeward side and .17445 in the windward side. The distribution of $v(\theta)$ as computed with the present technique and from the integration of (6) is shown in Fig. 5.

A word about the entropy distribution is in order here. As pointed out by Ferri (Ref. 7), the constant entropy lines on the unit sphere converge to a singular point on the leeward plane of symmetry. In our computation, the initial (arbitrary) distribution

of entropy is the one shown in Fig. 6, left-hand side. At the end of the computation, the constant entropy lines appear as in the right-hand side of the same figure. The singularity has been built up through a numerical procedure. Note that such a result is obtained using a very coarse mesh. To stress the point, Fig. 7 shows the building of the singularity by plotting several distributions of entropy on the body, at different steps in the computation.

The pressure distribution is shown in Fig. 8. In Fig. 9 the pressure distribution on the body is plotted as a function of φ for case (3) specified above. As expected, no sizeable difference exists among the present results, those obtained by a proper usage of Kopal's tables (Ref. 2), and the pressure distribution on a blunted cone at a certain distance from the nose. The latter results have been obtained analytically (by the technique of Ref. 13) and experimentally (Ref. 12).

VIII. LIMITATIONS OF THE INVISCID MODEL

To conclude, Fig. 10 shows the shock shapes for the four cases computed. In the first two cases, some points on the shocks as determined experimentally (Ref. 14) are shown by dots. The agreement between computation and experiment in the windward side is a proof of the soundness of the numerical procedure. The disagreement in the leeward side was expected. The present model is one of an inviscid flow. In reality, the viscous effects are important on a cone at an angle of attack, due to the three-dimensional behavior of the boundary layer (Ref. 17). By comparison of the numerical results with other data from Ref. 14, it appears that the difference in thickness in the leeward symmetry plane is of the order of the thickness of the viscous core.

In conclusion, the present computation, although self-consistent and accurate, is not yet adequate to describe the real motion, for lack of a realistic model of the gas. A more complicated model, in which viscous effects are taken into account, will be presented in a further communication.

REFERENCES

1. Courant, R. and Friedrichs, K. O., Supersonic Flow and Shock Waves, Interscience Publ., New York, p. 149, 1948.
2. Kopal, Z., Tables of Supersonic Flow Around Cones, MIT Dept. of Electrical Engr., Center of Analysis, Technical Rept. No. 1, Cambridge, Mass., 1947.
3. Stocker, P. M. and Mauger, F. E., Supersonic Flow Past Cones of General Cross-Section, J. Fluid Mech., Vol. 13, p. 383, 1962.
4. Holt, M. and Lee, S. C., Calculations of Supersonic Flow Past Yawed Cones by the Method of Integral Relations, Univ. California Rept. AS-64-7, Berkeley, Calif., 1964.
5. Stone, A. H., On Supersonic Flow Past a Slightly Yawing Cone, Part I, J. Math. and Physics, Vol. 27, p. 67, 1948.
6. Stone, A. H., On Supersonic Flow Past a Slightly Yawing Cone, Part II, J. Math. and Physics, Vol. 30, p. 200, 1951.
7. Ferri, A., Supersonic Flow Around Circular Cones at Angles of Attack, NACA Rept. 1045, 1951.
8. Woods, B. A., The Flow Close to the Surface of a Circular Cone at Incidence to a Supersonic Stream, Aero. Quart., Vol. 13, p. 115, 1962.
9. Gonor, A. L., Flow Over a Cone at an Angle of Attack for High Mach Number, ARS Journal, Vol. 32, p. 130, 1962.
10. Bulakh, B. M., On the Nonsymmetric Hypersonic Flow Around a Circular Cone, P.M.M., Vol. 26, p. 430, 1962.
11. Moretti, G. and Abbett, M., A Fast, Direct, and Accurate Technique for the Blunt Body Problem, CASL TR-583, Westbury, N. Y., January 31, 1966, AD 478119.

12. Zakkay, V., Pressure and Laminar Heat Transfer Results in Three-Dimensional Hypersonic Flow, WADC Tech. Report No. 58-182, September 1958.
13. Moretti, G., Sanlorenzo, E., Magnus, D. and Weilerstein, G., Flow Field Analysis of Reentry Configurations by a General Three-Dimensional Method of Characteristics, GASL Technical Report ASD-TR-727, Vol. III, Westbury, New York, Feb. 1962.
14. Tracy, R. R., Hypersonic Flow Over a Yawed Circular Cone, Graduate Aeronautical Labs., California Institute of Technology, CALCIT Memo No. 69, Pasadena, California, August 1, 1963.
15. Gonor, A. L., Location of Frontal Wave in Asymmetric Flow of Gas at High Supersonic Speed over a Pointed Body, ARS Journal, Vol. 30, No. 9, pp. 841-842, September 1960.
16. Courant, R., Friedrichs, K. O., and Lewy, H., Über die partielle Differentialgleichungen der mathematischen Physik, Mathematische Annalen, Vol. 100, pp. 32-74, 1928.
17. Moore, F. K., Three-Dimensional Boundary Layer Theory, Advances in Applied Mechanics, Vol. IV, pp. 159-228, 1956.

TABLE I

CONE AT AN ANGLE OF ATTACK

PROGRAM 3A - RUN NUMBER 11 ON 11/15/65

NA= 5, MA= 10, KA= 200, JA= 10, LA= -0, LB= -0, LC= -0, LD= -0, LE= -0, LF= -0

CONE HALF ANGLE= 1.00000E 01 DEGREES, ALPHA= 9.00000E 00 DEGREES, UO= 9.41000E 00, GAMMA= 1.40000E 00, STAB= 5.00000E 00

GUESS FOR SHOCK= 1.50000E 01, DELTH=10.00000E-03

EPS 1 TO 7

10.00000E-05 10.00000E-05 10.00000E-05 1.00000E 00 -0. -0. -0.

MACH NUMBER= 7.9529E 00, STANDOFF DISTANCE AT ZERO ANGLE OF ATTACK= 5.297662E-02

SHOCK ITERATION

	B	C	ERR(B)	ERR(C)	WPHI(1)	WPHI(2)
1	2.461303E-01	3.321745E-02	1.862368E-02	3.321745E-02	-1.309597E 00	1.309597E 00
1	2.495162E-01	2.785626E-02	3.385855E-03	-5.35110E -03	-1.263872E 00	6.172868E-01
2	2.494329E-01	2.802956E-02	-8.355565E-04	-5.791490E-04	-1.265693E 00	6.350081E-01
3	2.493270E-01	2.818341E-02	-1.223702E-04	1.340313E-04	-1.266798E 00	6.528740E-01
4	2.493209E-01	2.818864E-02	1.199171E-05	3.414042E-05	-1.266764E 00	6.527720E-01

GUESS FOR LEeward SHOCK

ENTROPY= 3.507286E-04

	THETA	U	V	RHO	P	M	V/U
1	2.775095E-01	9.320688E 00	-1.117585E 00	1.157315E 00	1.227396E 00	7.704015E 00	-1.199037E-01
2	2.675095E-01	9.331864E 00	-9.959939E-01	1.176324E 00	1.255712E 00	7.676840E 00	-1.067304E-01
3	2.575095E-01	9.341824E 00	-8.855479E-01	1.184930E 00	1.268592E 00	7.664706E 00	-9.479391E-02
4	2.475095E-01	9.350679E 00	-7.781474E-01	1.190135E 00	1.276401E 00	7.657418E 00	-8.321828E-02
5	2.375095E-01	9.358450E 00	-6.720345E-01	1.193427E 00	1.281347E 00	7.652828E 00	-7.181037E-02
6	2.275095E-01	9.365181E 00	-5.664531E-01	1.195387E 00	1.284294E 00	7.650102E 00	-6.048469E-02
7	2.175095E-01	9.370845E 00	-4.609509E-01	1.196286E 00	1.285646E 00	7.648854E 00	-4.918990E-02
8	2.075095E-01	9.375455E 00	-3.552157E-01	1.196241E 00	1.285578E 00	7.648916E 00	-3.788784E-02
9	1.975095E-01	9.379007E 00	-2.489646E-01	1.195278E 00	1.284130E 00	7.650253E 00	-2.654488E-02
10	1.875095E-01	9.381496E 00	-1.419143E-01	1.193348E 00	1.281227E 00	7.652938E 00	-1.512705E-02
11	1.775095E-01	9.382915E 00	-3.374197E-02	1.190322E 00	1.276682E 00	7.655715E 00	-3.596107E-03
12	1.750095E-01	9.383000E 00	-5.489177E-03	1.190135E 00	1.276400E 00	7.657418E 00	-5.850130E-04
13	1.746970E-01	9.383051E 00	-1.912078E-03	1.190133E 00	1.276397E 00	7.657421E 00	-2.037810E-04
14	1.745407E-01	9.383032E 00	-1.213769E-04	1.190132E 00	1.276396E 00	7.657422E 00	-1.293583E-05
15	1.745510E-01	9.383002E 00	-9.362918E-06	1.190132E 00	1.276396E 00	7.657422E 00	-9.978596E-07
16	1.745303E-01	9.383002E 00	-2.361673E-06	1.190132E 00	1.276396E 00	7.657422E 00	-2.516969E-07
17	1.745302E-01	9.383002E 00	-6.113560E-07	1.190132E 00	1.276396E 00	7.657422E 00	-6.515570E-08

GUESS FOR WINDWARD SHOCK

ENTROPY= 3.796395E-01

	THETA	U	V	RHO	P	M	V/U
1	2.211322E-01	8.804279E 00	-9.048338E-01	3.670907E 00	9.027304E 00	4.770006E 00	-1.027720E-01
2	2.111322E-01	8.813328E 00	-7.158011E-01	3.749749E 00	9.299903E 00	4.745320E 00	-8.121803E-02
3	2.011322E-01	8.820486E 00	-5.271317E-01	3.808492E 00	9.504506E 00	4.727313E 00	-5.976221E-02
4	1.911322E-01	8.825757E 00	-3.353668E-01	3.848063E 00	9.643047E 00	4.715363E 00	-3.799865E-02
5	1.811322E-01	8.829111E 00	-1.374108E-01	3.866945E 00	9.709363E 00	4.709711E 00	-1.556338E-02
6	1.761322E-01	8.829798E 00	-3.403503E-02	3.870023E 00	9.720178E 00	4.708793E 00	-3.854565E-03
7	1.749822E-01	8.829840E 00	-7.506550E-03	3.870216E 00	9.720859E 00	4.708735E 00	-8.501343E-04
8	1.745697E-01	8.829842E 00	-8.266442E-04	3.870225E 00	9.720890E 00	4.708732E 00	-9.361936E-05
9	1.745502E-01	8.829842E 00	-4.084060E-04	3.870225E 00	9.720890E 00	4.708732E 00	-4.625292E-05
10	1.745404E-01	8.829842E 00	-1.992617E-04	3.870225E 00	9.720890E 00	4.708732E 00	-2.256685E-05
11	1.745355E-01	8.829842E 00	-9.468329E-05	3.870225E 00	9.720890E 00	4.708732E 00	-1.072310E-05
12	1.745331E-01	8.829842E 00	-4.239250E-05	3.870225E 00	9.720890E 00	4.708732E 00	-4.801049E-06
13	1.745319E-01	8.829842E 00	-1.624671E-05	3.870225E 00	9.720890E 00	4.708732E 00	-1.839978E-06
14	1.745313E-01	8.829842E 00	-3.173722E-06	3.870225E 00	9.720890E 00	4.708732E 00	-3.594313E-07
15	1.745312E-01	8.829842E 00	-1.539592E-06	3.870225E 00	9.720890E 00	4.708732E 00	-1.743623E-07
16	1.745311E-01	8.829842E 00	-7.225265E-07	3.870225E 00	9.720890E 00	4.708732E 00	-8.182780E-08

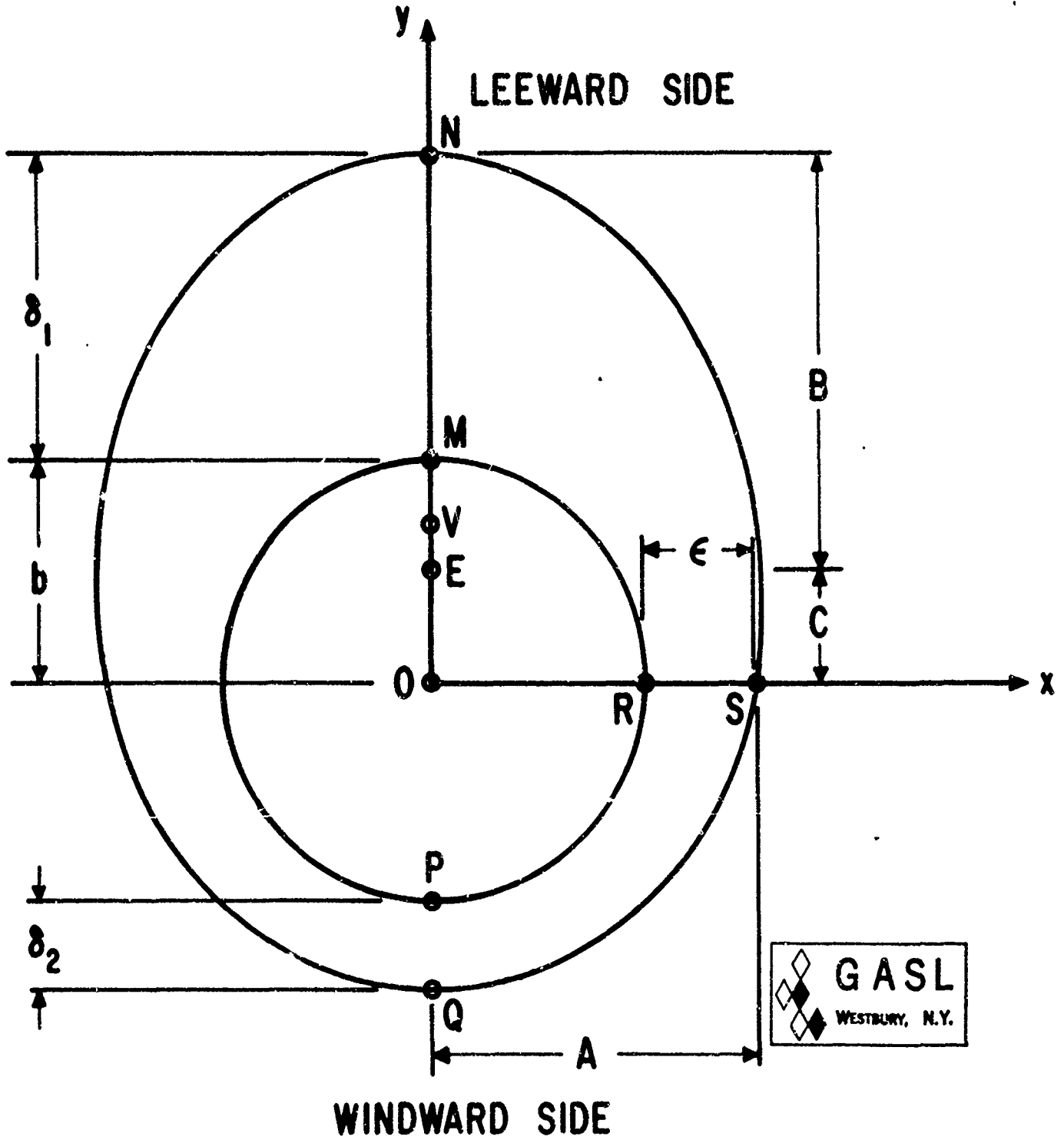


FIG. 1 SCHEMATIC OF CONE AND ASSUMED SHOCK GEOMETRY

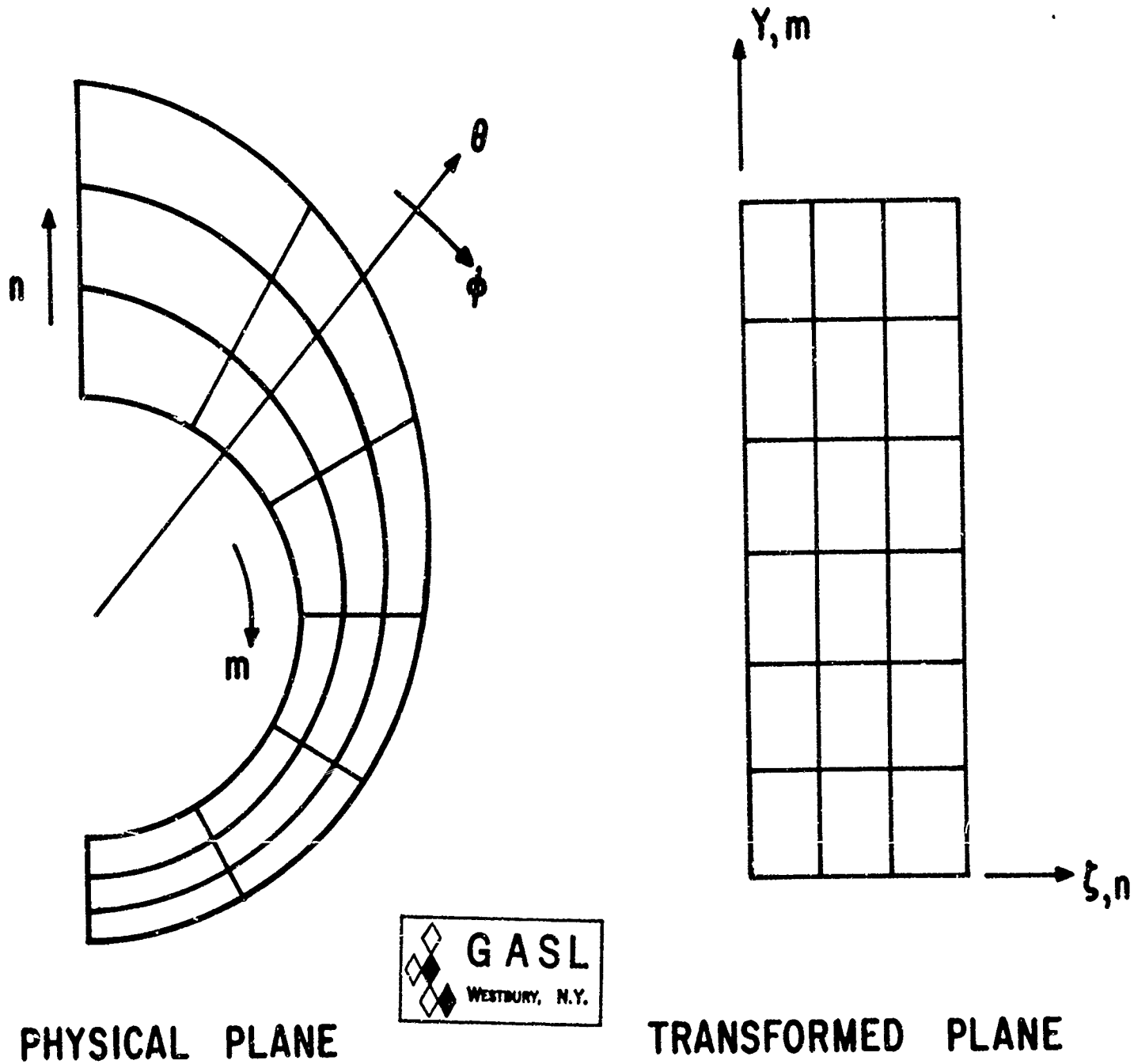
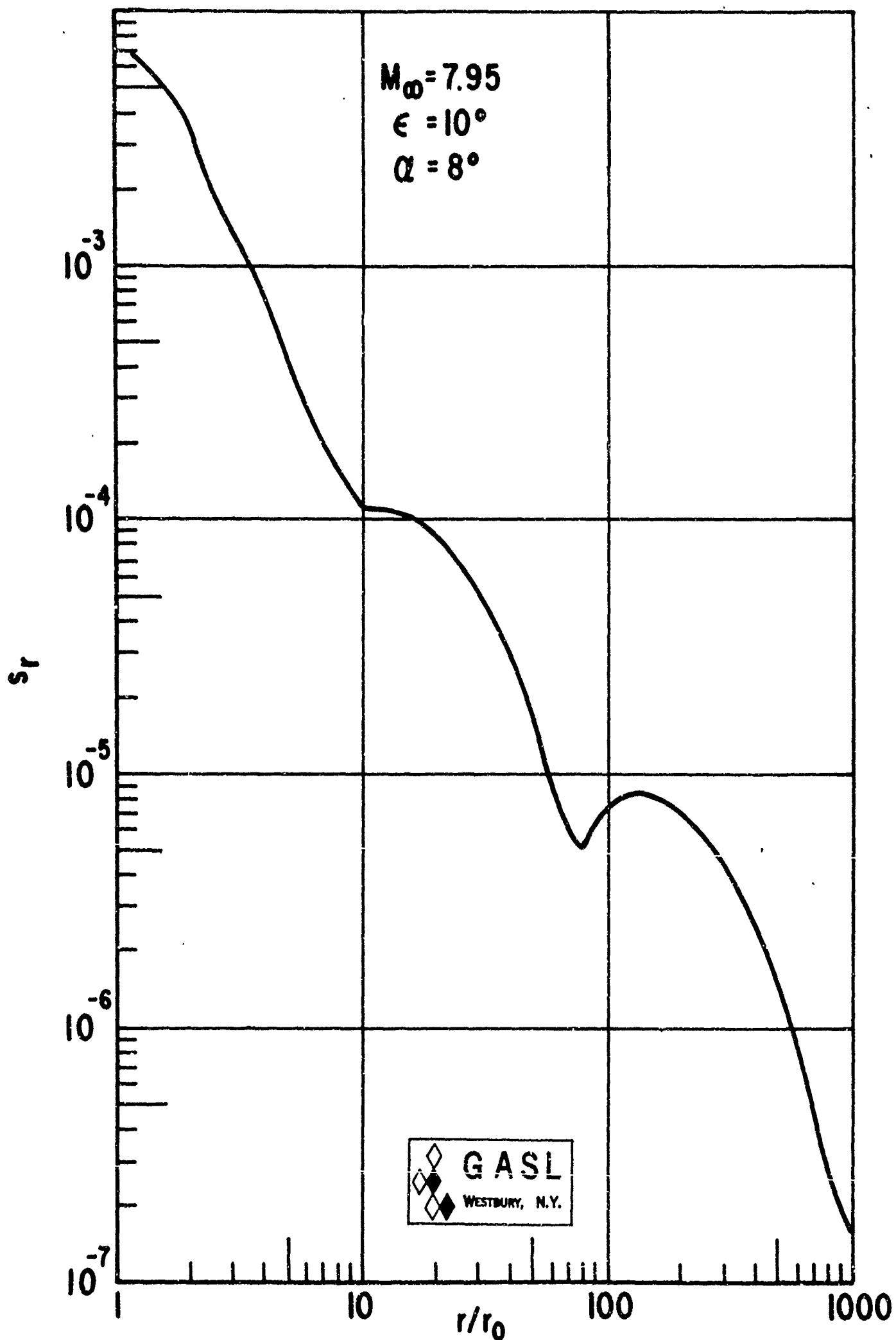


FIG. 2 SCHEMATIC OF MESH

FIG. 3 RANGE OF $\Delta\theta/\Delta r$ AS A FUNCTION OF RADIUS

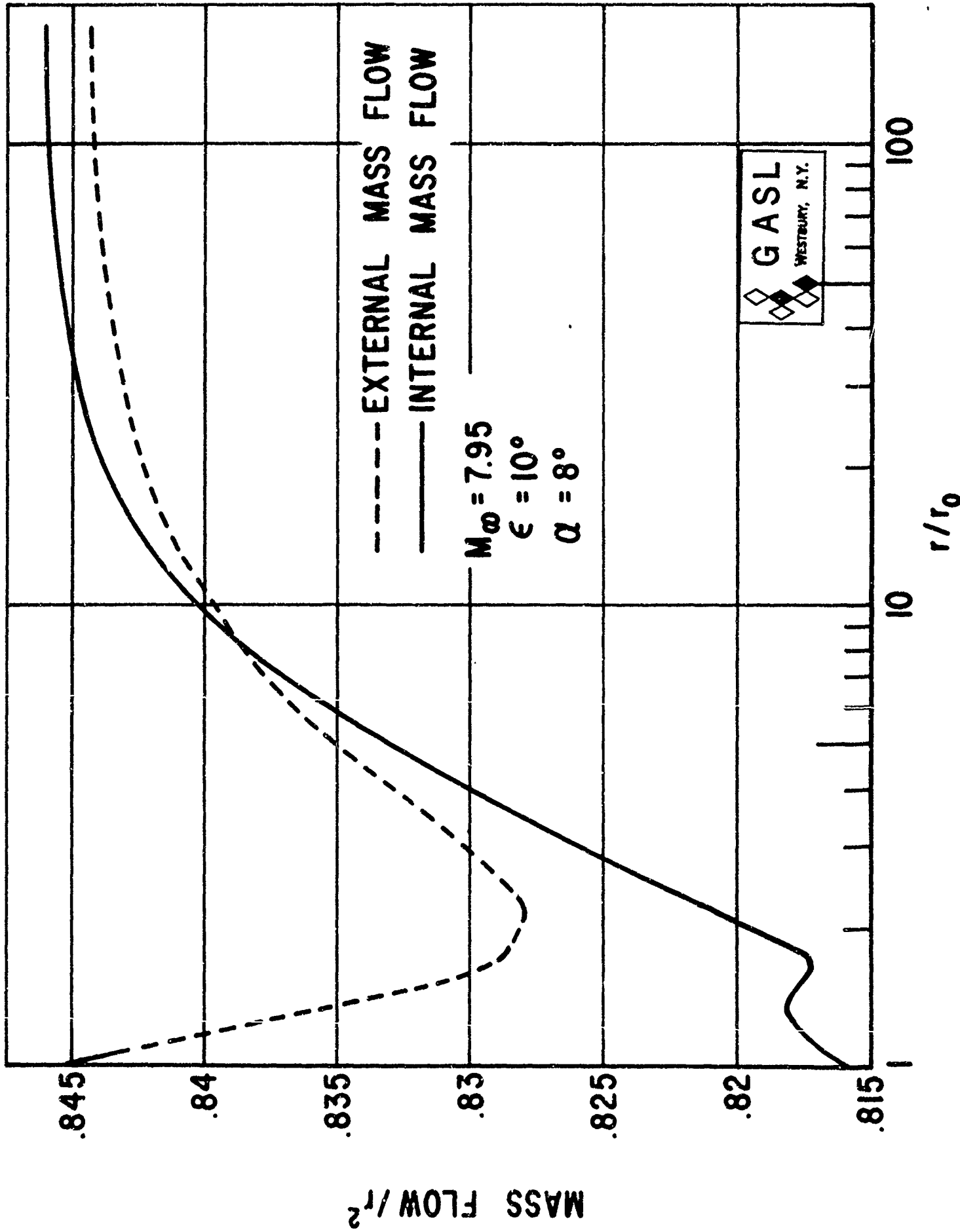


FIG. 4 MASS FLOW AS A FUNCTION OF RADIUS

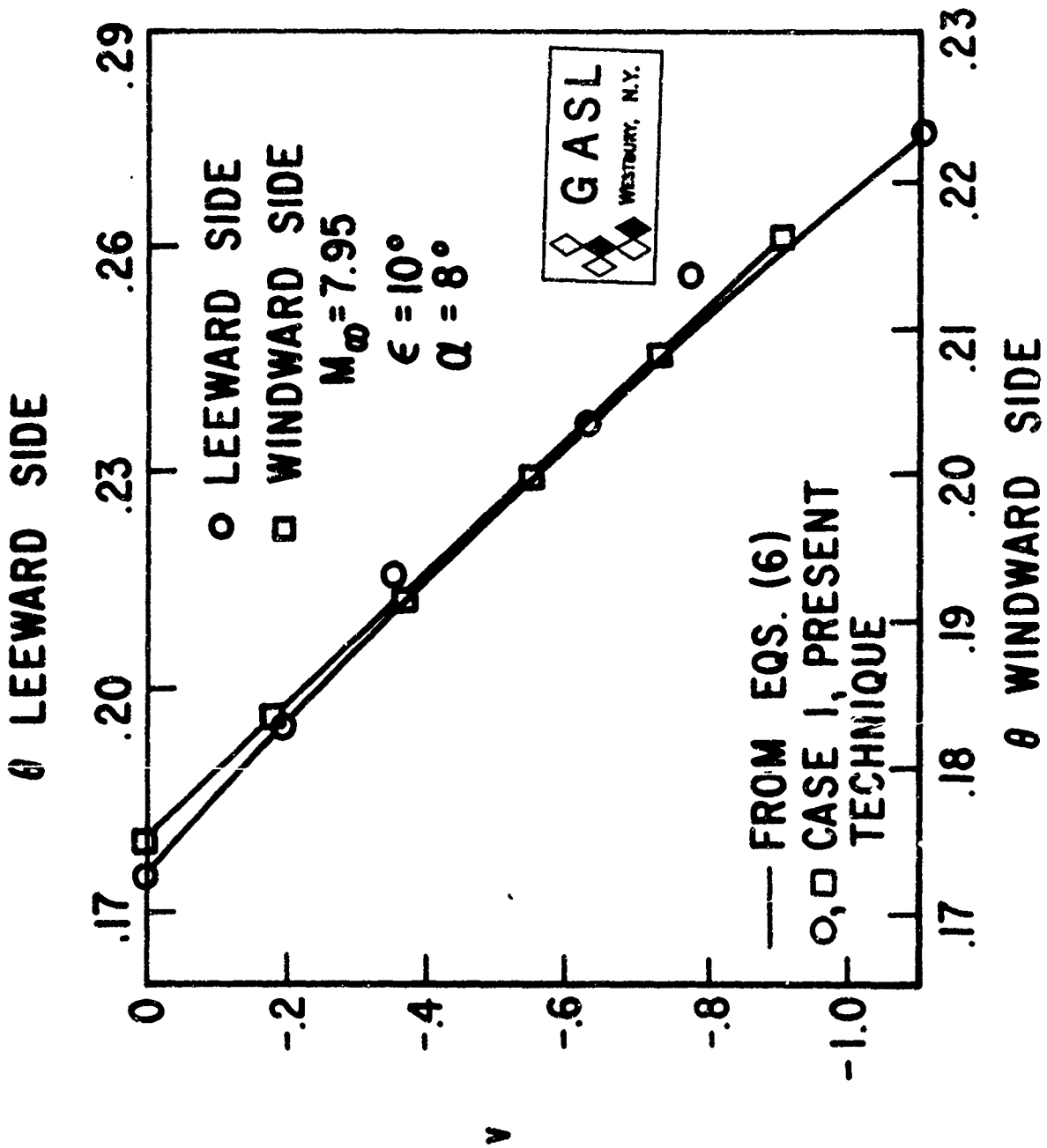


FIG. 5 VELOCITY DISTRIBUTION IN SYMMETRY PLANE DETERMINED FROM COMPUTED VALUES OF w_{ϕ}

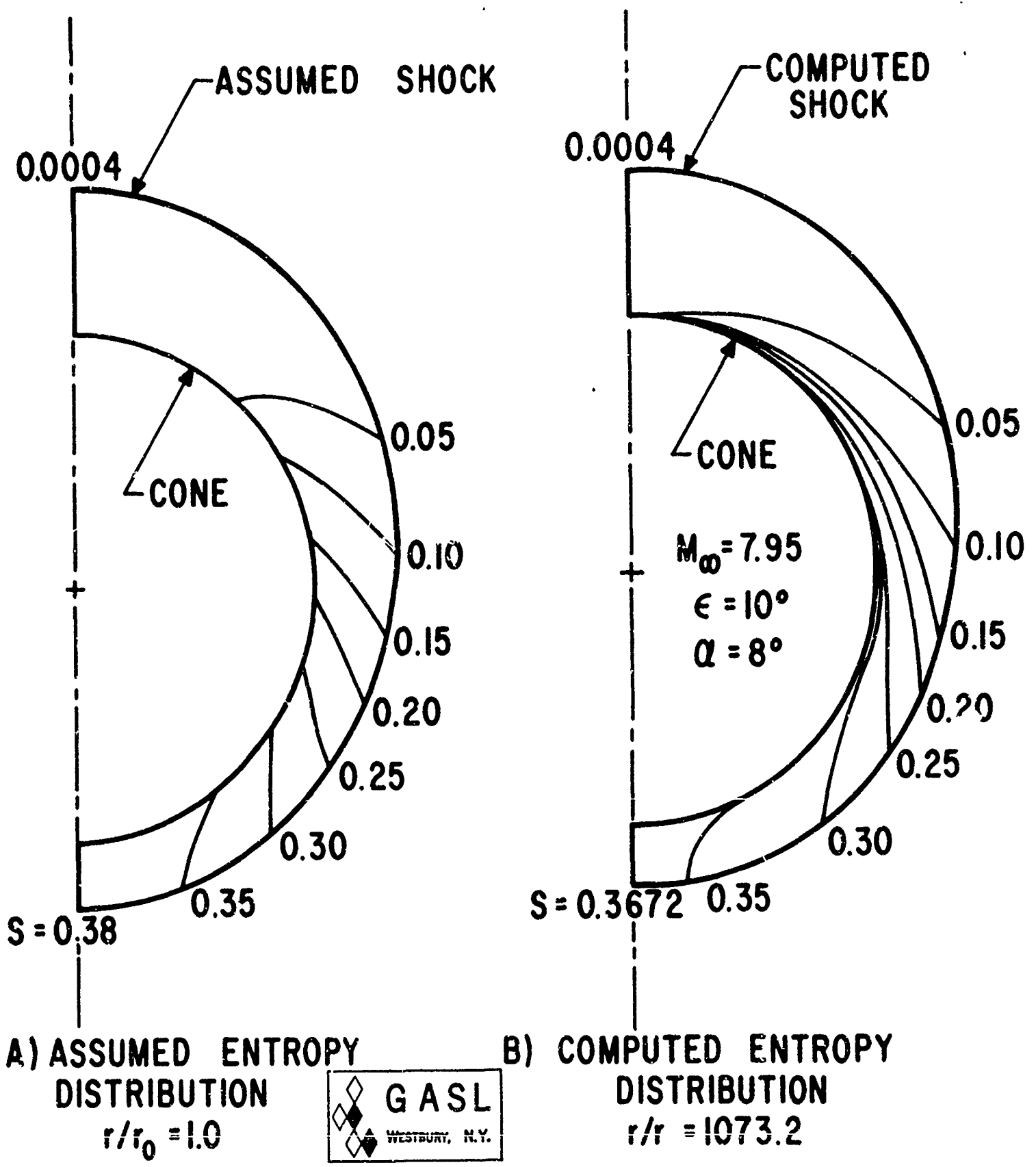


FIG. 6 ASSUMED AND COMPUTED ENTROPY DISTRIBUTION

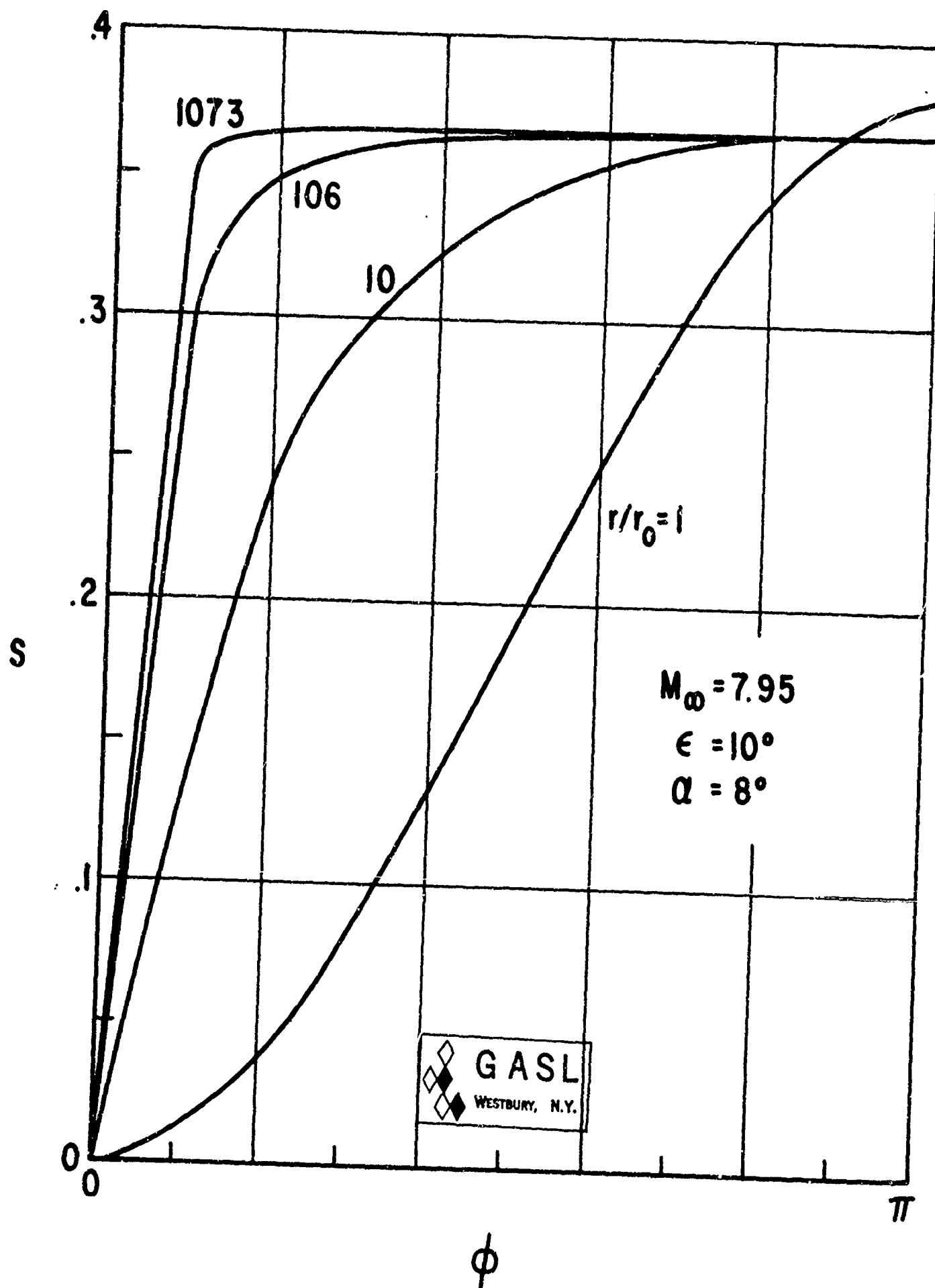


FIG. 7 ENTROPY DISTRIBUTION ON BODY AT VARIOUS VALUES OF r/r_0

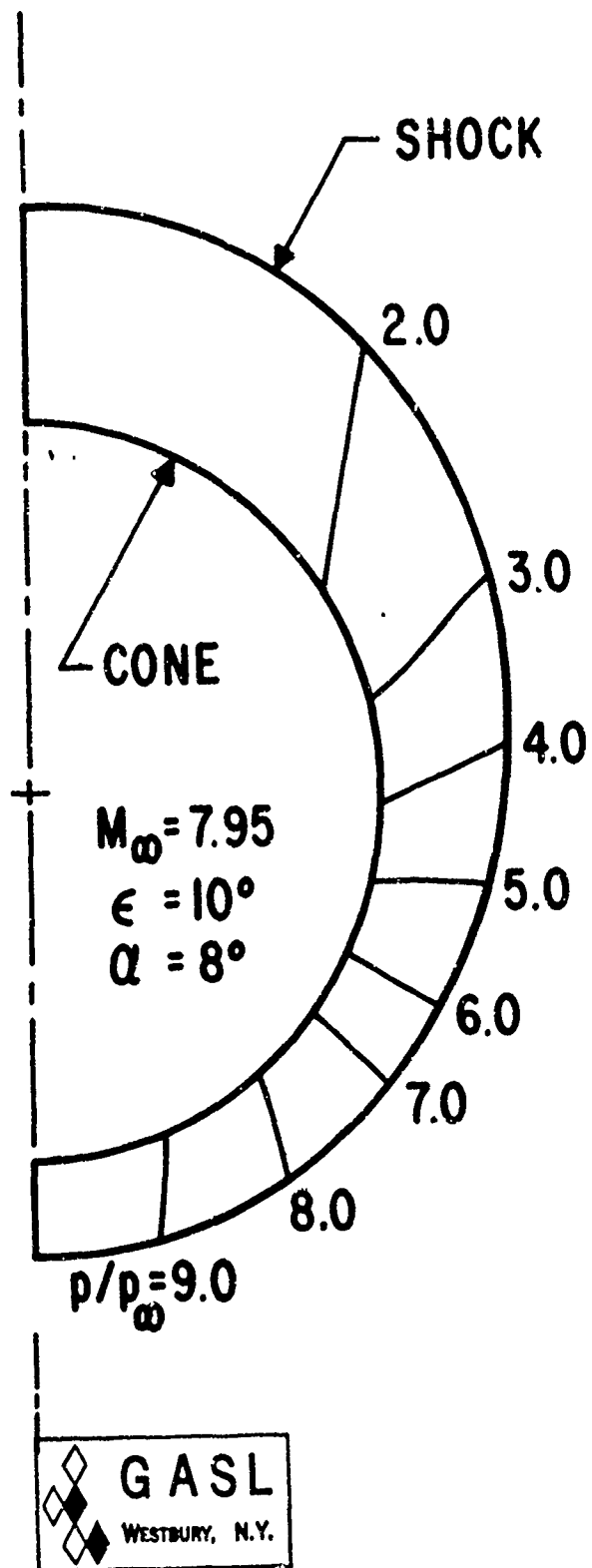
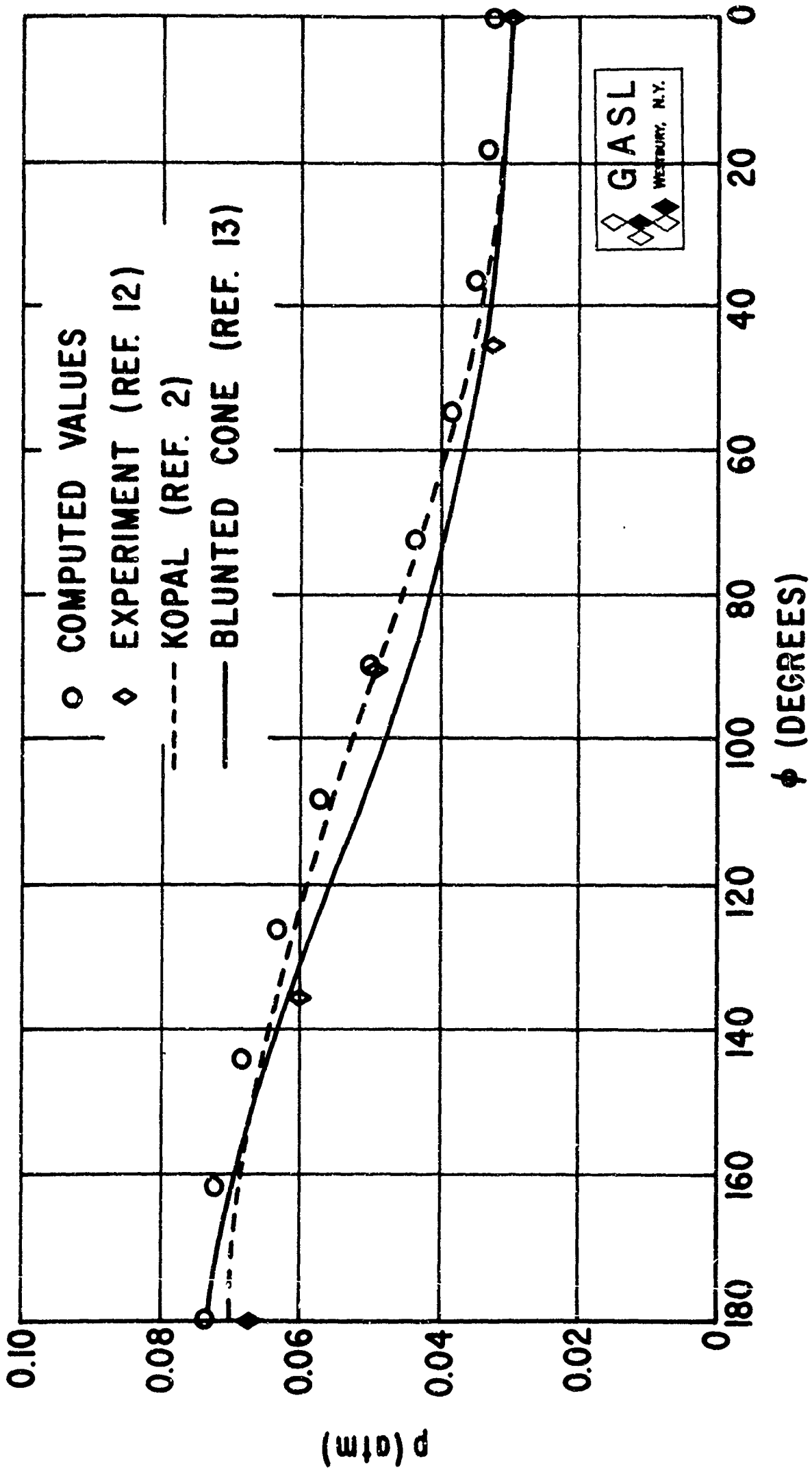
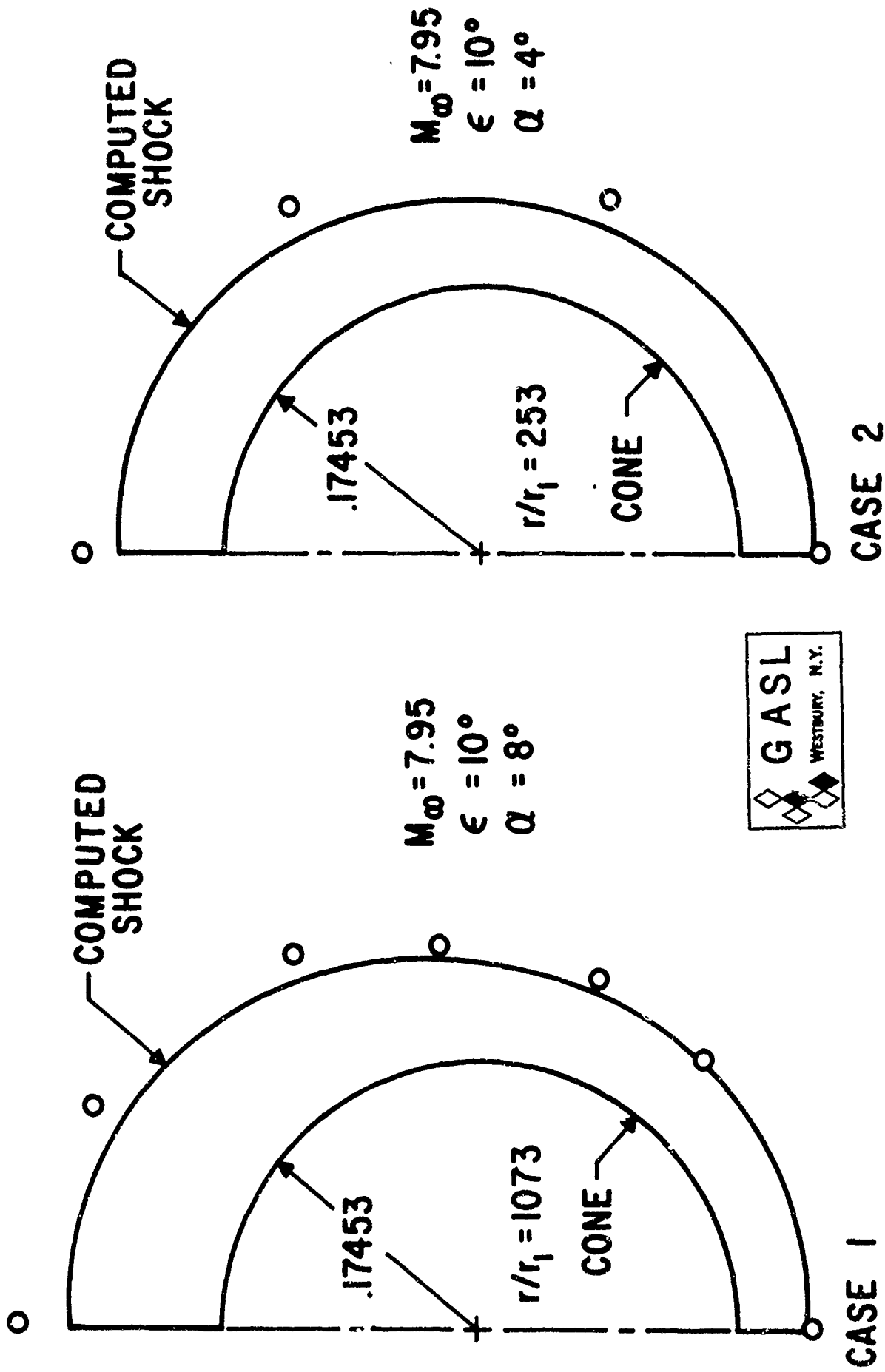


FIG. 8 PRESSURE DISTRIBUTION CASE I



GASL
WESTBURY, N.Y.

FIG. 9 PRESSURE ON BODY, $M_\infty = 8$, $\epsilon = 20^\circ$, $\alpha = 5^\circ$



EXPERIMENTAL VALUES (REF. 14)

FIG. 10a COMPUTED SHOCK SHAPES FOR CASES 1,2

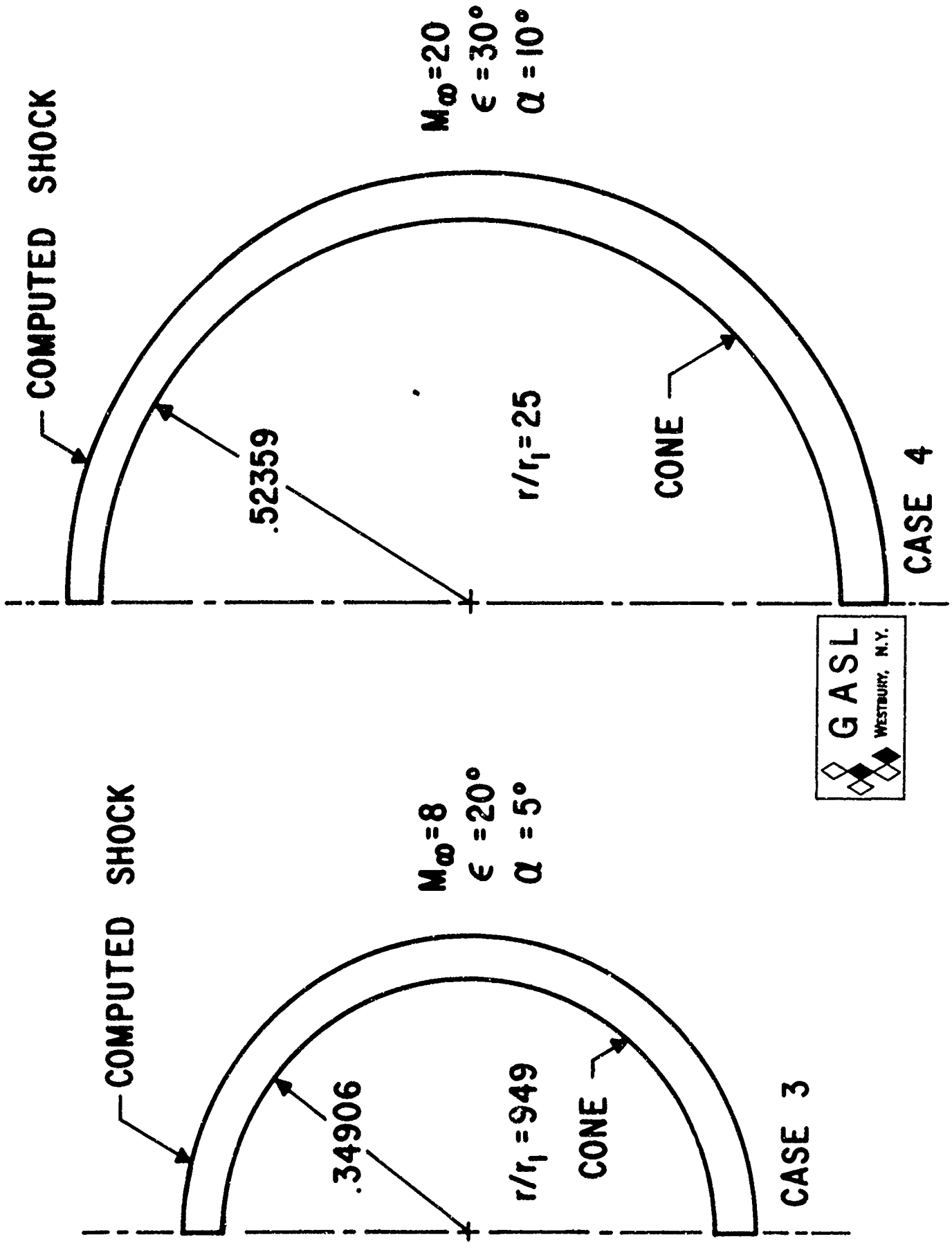


FIG. 10b COMPUTED SHOCK SHAPES FOR CASES 3, 4

DISTRIBUTION LIST "A"

CONTRACT SD-149

SUPPLEMENT #6

ORGANIZATION

NO. OF CYS.

DOD

Advanced Research Projects Agency
The Pentagon, Rm. 2B-261
Washington, D.C. 20301
Attn: Technical Information Office (25-8030-2) 1
Dr. B. Fisher (25-8030-3) 1
Mr. V. S. Kupelian (95-8030-4) 1
Mr. R. Zirkind (25-8030-5) 1
Mr. C. McLain (25-8030-6) 1
Mr. W. A. Van Zeeland (95-8030-80) 1
Dr. P. L. Auer (95-8030-81) 1

Director (45-8030-7) 1
Weapons Systems Evaluation Group
Washington, D.C. 20305

Defense Documentation Center (25-8030-8) 20
Cameron Station
Alexandria, Va.

ARMY

U.S. Army Missile Command
Redstone Arsenal, Alabama 35809
Attn: AMSMI-RFE (95-8030-9) 1
AMSMI-RBLD (95-8030-82) 5